UC Berkeley
UC Berkeley Previously Published Works

Title
Lead halide perovskite nanowires stabilized by block copolymers for Langmuir-Blodgett assembly

Permalink
https://escholarship.org/uc/item/8gg4x5t7

Journal
Nano Research, 13(5)

ISSN
1998-0124

Authors
Liu, Hao
Siron, Martin
Gao, Mengyu
et al.

Publication Date
2020-05-01

DOI
10.1007/s12274-020-2717-9

Peer reviewed

TABLE OF CONTENTS (TOC)

Langmuir-Blodgett assembly of lead halide Perovskite nanowires stabilized by block copolymers
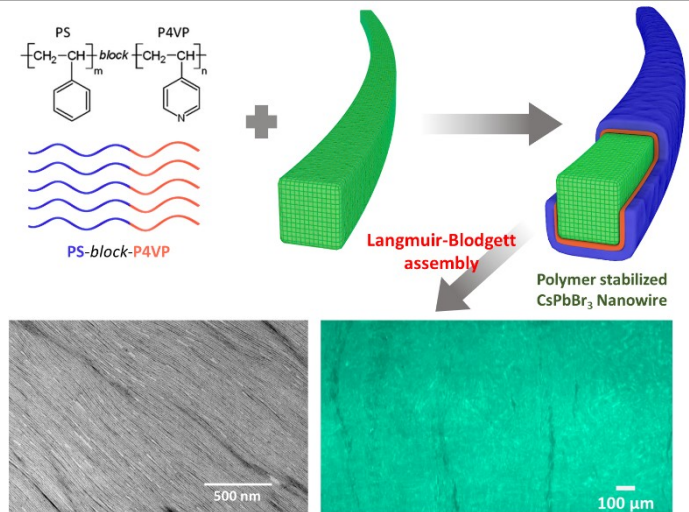
Hao Liu[1,3], Martin Siron[2], Mengyu Gao[2,3], Dylan Lu[1,3], Yehonadav Bekenstein[1,3,4], Dandan Zhang[1,3], Letian Dou[1,3], A. Paul Alivisatos[1,2,3,4], and Peidong Yang[1,2,3,4]*

[1] Department of Chemistry and [2]Department of Materials Science and Engineering, University of California, United States

[3]Materials Science Division, Lawrence Berkeley National Laboratory, United States

[4]Kavli Energy NanoScience Institute, United States

Page Numbers. The font is

ArialMT 16

(automatically

inserted by the

publisher)

An amphiphilic block copolymer, PS-P4VP, was introduced to chemically modify the surface of colloidal $CsPbBr_3$ nanowires. Taking advantage of the stability enhancement, we further applied a modified Langmuir-Blodgett technique to assemble monolayers of highly aligned nanowires and studied their anisotropic optical properties.

Lead halide perovskite nanowires stabilized by block copolymers for Langmuir-Blodgett assembly

Hao Liu[1,3,†], Martin Siron[2], Mengyu Gao[2,3], Dylan Lu[1,3], Yehonadav Bekenstein[1,3,4], Dandan Zhang[1,3], Letian Dou[1,3], A. Paul Alivisatos[1,2,3,4], and Peidong Yang[1,2,3,4](✉)

[1]Department of Chemistry and [2]Department of Materials Science and Engineering, University of California, Berkeley, California

94720, United States

[3]Materials Science Division, Lawrence Berkeley National Laboratory, Berkeley, California 94720, United States

[4]Kavli Energy NanoScience Institute, Berkeley, California 94720, United States

[†]Center for Advanced Low-dimension Materials, College of Materials Science and Engineering, Donghua University, Shanghai 201620, China

ABSTRACT

The remarkable optoelectronic properties of lead halide perovskites (LHPs) has prompted active research outputs on enhancing, tuning and improving this material on the fundamental and device level. Colloidal nanostructures of such materials display enhanced optoelectronic properties. Especially, highly orientated, one dimensional (1D) LHPs nanowires show a strong degree of anisotropy in their optical behavior. Unfortunately, LHPs are very sensitive to their external environment due to their ionic nature, and low dissociation energy. This limits their use in large-scale practical applications. We introduce an amphiphilic block copolymer, polystyrene-block-poly(4-vinylpyridine) (PS-P4VP), to chemically modify the surface of colloidal $CsPbBr_3$ nanowires. The resulting core-shell structure shows enhanced photoluminescent emission and better colloidal stability against water. Taking advantage of the stability enhancement, we further applied a modified Langmuir-Blodgett technique to assemble monolayers of highly aligned nanowires, and to study their anisotropic optical properties.

KEYWORDS

Nanowires, anisotropic optical properties, aligned monolayer, lead halide perovskites, stability enhancement.

1 Introduction

All-inorganic cesium lead halide perovskites $CsPbX_3$ (X = I, Br or Cl) have demonstrated great potential for a wide range of ~~applications, such~~ as photodetection [1], efficient backlight displays [2], light-emitting diodes (LED) [3], lasers [4] and photovoltaic devices [5]. Their significance is due to the exceptional light harvesting properties along with their significantly facile synthesis [6]. Among all colloidal nanostructures, 1D nanowires possess the highest shape anisotropy, leading to enhanced quantum and dielectric confinement effects [7, 8]. Oriented assembly of 1D nanostructures was widely investigated for anisotropic optoelectronic and nonlinear optical applications [9]. Langmuir-Blodgett (LB) assembly is a feasible technique to assemble a large-area monolayer of nanostructures with high degree of orientation at a water/air interface [10, 11], which can then be easily transferred to various solid substrates. Therefore, it provides us a platform to study the optical or optoelectronic properties of such aligned 1D nanowires.

However, unlike other conventional inorganic semiconducting compounds (e.g., indium pnictides, cadmium chalcogenides, GaAs), LHPs are highly ionic crystals with low dissociation energy (e.g., 0.25 eV per atom of $CsPbBr_3$ → CsBr + $PbBr_2$ [12]). As a result, they show poor stability under certain conditions [6]. Specifically, structure decomposition of LHPs nanocrystals can be simply induced, or accelerated, by many stimuli, including moisture, polar solvents, light, and heat [13].

Address correspondence to Peidong Yang, p_yang@berkeley.edu

The poor stability of LHPs has been one of the major concerns for their large-scale production and applications. One layer of protection for colloidal nanocrystals is traditionally provided by the presence of long-chain surfactants (e.g., carboxylic acids and alkylamines) on the nanocrystals surface [14] . De Roo *et al.* found that the binding between such surfactants and the LHPs surfaces is weak and highly dynamic. This may result in ligands loss during standard postsynthetic purification processes [15], and thus, poor colloidal stability and a decline in optoelectronic properties.

To overcome this challenge, two main postsynthetic treatments are being explored by the community: macroscale immobilization in water-resistant polymer matrices [16, 17], and chemical surface modification by ligands with strong affinity for the nanocrystal's surface [18]. For instance, Raja *et al.* succeeded in immobilizing $CsPbBr_3$ nanocrystals into presynthesized hydrophobic polymeric bulk matrices [17]. In the resulting composites, water and light stability were both enhanced by orders of magnitude on the time scale. However, such treatment eliminates the physical contact of the nanocrystals with external environment. It also eliminates the potential for self-assembly, and prevents further applications that require mass or electron transport [6]. To realize the LB assembly of LHP nanowires, the second type of post-synthetic treatment described above should be applied. A straightforward solution is to build up a core-shell structure to

provide protection to the NW core and prevent severe bundling. Such a shell material should have strong yet non-destructive interactions with the surface of the LHP nanocrystals. Additionally, the shell material should do no harm to the optoelectronic properties of the core.

Here, we report the employment of an amphiphilic block copolymer polystyrene-*block*-poly-(4-vinylpyridine) (PS-P4VP), as the shell material to perform the postsynthetic treatment on 1D $CsPbBr_3$ nanowires [19, 20] (Figure 1a). We hypothesize that the multidentate P4VP block will serve as an anchor to the surface of $CsPbBr_3$ NWs, while the hydrophobic polystyrene block will provide significant water protection [16]. This hypothesis is based on the idea that the lone electron pairs of the nitrogen atoms in the pyridine rings are able to coordinate the empty 6p orbitals of Pb^{2+}, as suggested by theoretical simulation and experimental observations [21, 22]. Thus, the lead rich surfaces of the nanowires [23] will allow for the formation of the protective polymeric shell.

2 Experimental

2.1 Post-synthetic treatment of $CsPbBr_3$ nanowires

The synthetic procedure of $CsPbBr_3$ nanowires followed previous papers with slight modification (see details in Supporting Information) [20, 24]. PS-P4VP was dissolved in chloroform with varying concentrations (4 mg/mL, 2 mg/mL and 1 mg/mL). 1 mL of the as-synthesized NWs stock solution was diluted with 9 mL dried toluene. 1 mL PS-P4VP chloroform solution with a certain concentration was gradually added under gentle stirring at room temperature. The turbid NWs suspension turned translucent during the polymer solution addition.
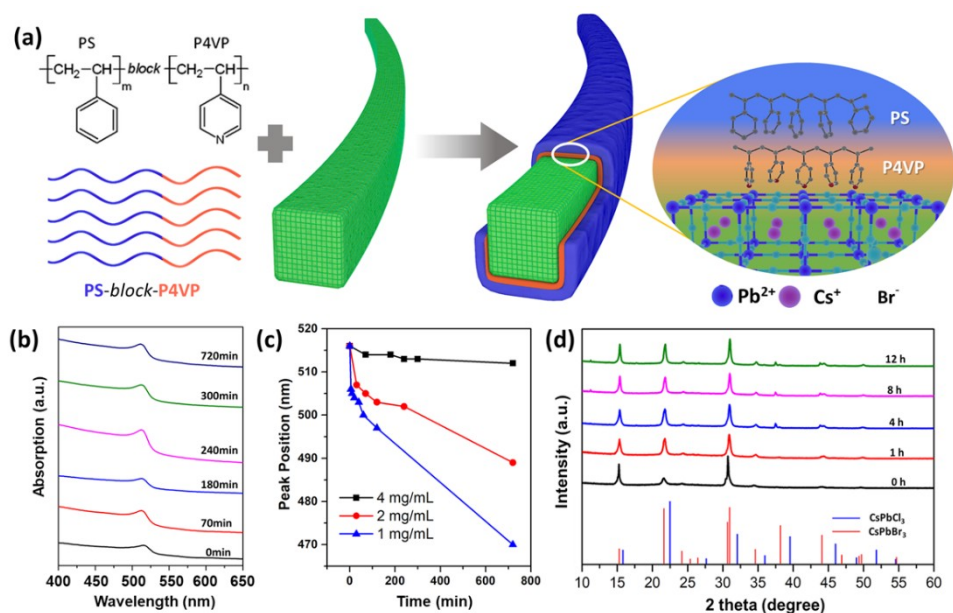
Figure 1(a) Schematic representations of the chemical structure of PS-P4VP, the post-synthetic treatment process and the final core-shell configuration of the $CsPbBr_3$ NWs. (b) Time evolution of the optical absorption spectra of $CsPbBr_3$ NWs toluene suspension treated by 4 mg/mL PS-P4VP chloroform solution (toluene : chloroform = 9: 1 in volume). (c) Time evolution of the optical absorption peak position with varying polymer concentrations, i.e. 1 mg/mL, 2 mg/mL and 4 mg/mL in chloroform (toluene : chloroform = 9: 1 in volume). (d) Time-evolutionary XRD patterns of the $CsPbBr_3$ NWs treated with 4 mg/mL PS-P4VP chloroform solution. The red and blue lines at the bottom are standard XRD patterns of orthorhombic phases of $CsPbBr_3$ and $CsPbCl_3$.

2.2 Langmuir-Blodgett assembly of polymer-coated $CsPbBr_3$ nanowires

5 mL of the polymer-coated $CsPbBr_3$ NWs suspension (toluene/hexanes = 1/1 in volume, ~ 8 mg/mL) was spread dropwise with a glass syringe onto the acetonitrile/water surface (55 vol.% acetonitrile in water) of a Langmuir-Blodgett trough (KSV NIMA KN 2002, Biolin Scientific). The NWs formed a greenish layer on the solvent surface, which was subsequently compressed by two barriers with a speed of 10 cm^2/min (the width of the trough is 7.5 cm). The surface pressure was monitored with a Wilhelmy plate during the compression. The film was compressed until different surface pressures were reached, and then deposited to various substrates (copper grids and quartz slides) for further characterization. Typically, the substrates were dipped and then pulled vertically through the film with a speed of 1.5 mm/min.

2.3 Physical characterization

Powder X-ray diffraction (XRD) patterns were collected on a Bruker AXS D8 Advance diffractometer with a Cu K_α source. The NWs samples were centrifuged out from solutions and dried in vacuum before the XRD test. Glass slides were used to hold the powder samples. Background signals from glass were subtracted accordingly. The transmission electron microscopy (TEM) images were taken by a Hitachi H-7650 TEM at an accelerating

voltage of 120 kV. All the TEM samples were thoroughly dried in vacuum before TEM test. It needs to be emphasized that the polymer-treated NWs were centrifuged first, and then re-dispersed in toluene before preparing TEM grids. Ultraviolet-visible light (UV-Vis) absorption spectra were collected by a Shimudzu UV-3010 PC UV-VIS-IR scanning spectrophotometer equipped with a Shimadzu ISR-3100 integrating sphere. Photoluminescence spectra and PL quantum yield were measured on a Horiba Jobin-Yvon FluoroLog 2 spectrofluorometer.

medium polarity impact the integrity of the $CsPbBr_3$ perovskite structure. For example, in pure
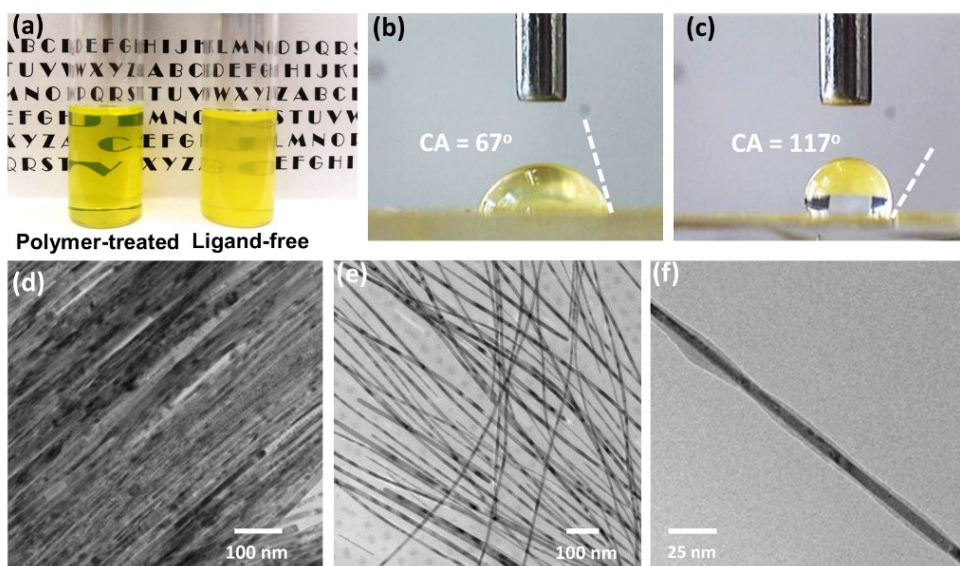
Figure 2 (a) Picture of the polymer-treated NWs solution and surface ligand-free NWs solution. Both solutions are toluene mixed with 10 % chloroform. (b) Contact angle measurements on the drop-cast film of the ligand-free NWs and (c) polymer-treated NWs. (d) TEM images of the bundles of ligand-free NWs and (e) well-dispersed polymer-treated NWs. (f) An enlarged TEM image showing the thin shell of PS-P4VP on the surface of a single NW.

chloroform, the ligand-free NWs quickly underwent a chemical transformation from $CsPbBr_3$ to $CsPb_2Br_5$, a non-perovskite structure (see Figure S1) [25]. When placing the ligand-free NWs in toluene with 10 vol. % chloroform, the perovskite structure remained intact, but a significant blue-shift of the ultraviolet-visible (UV-Vis) band edge absorption peak was observed over time (Figure S2). This is due to the slow decomposition of chloroform, generating active chlorine species that replace bromide atoms in the ligand-free NWs (see WAXD patterns in Figure S3) [20].

The fragile surface of LHP provides a challenge. Unfortunately, the best solvent to dissolve PS-P4VP is chloroform. Thus, the polymer concentration should be well-tuned to minimize side effects from chloroform.

spectra still occurred (Figure S4). However, when using a PS-P4VP solution of 4 mg/mL concentration or higher, the blue-shift was negligible for over 12 hours (Figure 1b). The concentration effect is summarized in Figure 1c. It is reasoned that the polymer solution with higher concentration is able to provide more polymeric coverage to the NWs, protecting the core from chlorine species. Moreover, WAXD patterns of the NWs treated with 4 mg/mL polymer solution showed no obvious shift over 12 hours (Figure 1d), confirming that the treatment did provide the protection against anion exchange and the PS-P4VP shell did not induce a structural change at high polymer concentration. We examined the PL emission spectra evolution of the ligand-free NWs solution treated with 4 mg/mL
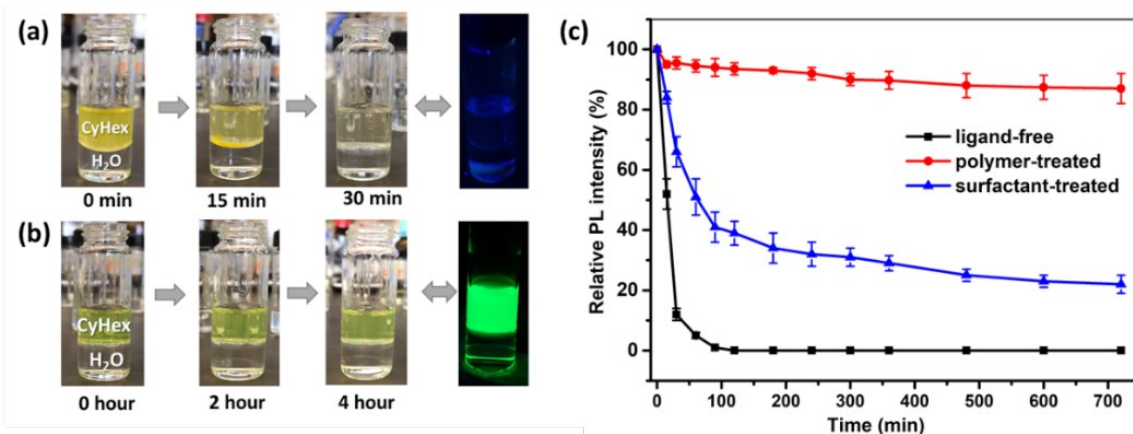
Polymer solutions of different concentrations were added dropwise into the ligand-free NWs suspension in toluene (10 % total chloroform by volume) under stirring. It was found that at low polymer concentration (i.e., 1 mg/mL and 2 mg/mL), a blue-shift in the absorption

PS-P4VP chloroform solution (Figure S5a) and pure chloroform as a control (Figure S5b). As shown in Figure S5, the normalized PL intensity of the polymer-treated NWs is 16 times stronger than the control. The PLQY of the NWs after the treatment was 11.2 % ± 0.8

%. Zuo *et al.* found that the P4VP homopolymers possess the ability to passivate the surface trap states at the grain boundaries of hybrid perovskite films, and thus, the optoelectronic properties and overall photovoltaic performance were promoted [26]. In terms of CsPbBr$_3$ NWs, due to the large surface-to-volume ratio, the shallow surface traps may cause a significant reduction in the PLQY. Hence, we can attribute PL enhancement of the polymer-coated NWs to the passivation of these sites by the P4VP block.

Figure 3(a) Pictures of the ligand-free NWs suspension in cyclohexane and (b) the PS-P4VP treated NWs solution at different time points after shaking together with an aqueous layer. (c) Time evolution of the relative PL intensity for three samples in the colloidal stability tests: ligand-free, PS-P4VP treated, and small ligands treated NWs.

It is well known that the colloidal stability is hindered by aggregation and sedimentation phenomena, which are driven by the colloids' tendency to reduce their surface energy. Aggregation is a common and bothersome problem in the surfactant-assisted synthesis of nanowires. As shown in Figure 2a, the ligand-free NWs suspension is turbid, suggesting severe bundling in the solution. On the contrary, the polymer-treated NWs solution is more translucent. The surface chemistry of NWs can also be evaluated by contact angle measurements. In Figure 2b and 2c, contact angles of a deionized water droplet on the flattened powers of ligand-free NWs and polymer-treated NWs are 67° and 117°, respectively, indicating that the copolymer treatment successfully modified the surface of NWs to be more hydrophobic. Morphologies of the ligand-free NWs and polymer-coated NWs were examined by TEM. The ligand-free NWs prefer to form aggregates (Figure 2d), while the polymer-treated NWs tend to be well-dispersed and separated from each other (Figure 2e). In Figure 2f, we can see the single NW is encapsulated by a thin layer (~2 nm) of
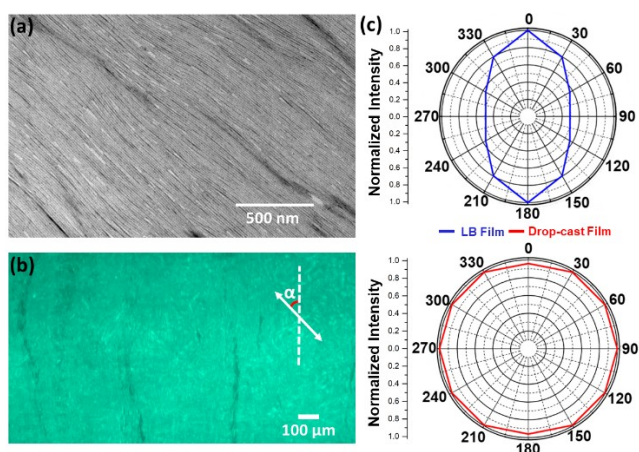
PS-P4VP (more TEM images of polymer-coated NWs are available in Figure S6).

To investigate the resistance of the colloidal NWs to water, we placed a thick layer of water under a layer of NWs in cyclohexane and shook it by hand to mix the two phases (Figure 3a and Figure 3b). During the first 30 min, the ligand-free NWs quickly precipitated out and the solution lost its characteristic yellowish color (Figure 3a). This is due to the dissolution of the CsPbBr$_3$ in water through the water/oil interface. The PL emission diminished exponentially with time, and became negligible after 60 min (Figure 3c). On the other hand, the polymer-coated NWs showed very good colloidal stability against

water. Both the solution color and PL emission kept intact during the first 4 hours (Figure 3b). Moreover, the PL intensity only dropped ~ 10% overnight (Figure 3c). We also compared this surface treatment to $CsPbBr_3$ NWs post-treated by small molecule ligands (a mixture of oleic acid, oleylamine and $PbBr_2$) a process developed in our previous NW studies [20]. As displayed in Figure 3c, the PL intensity also dropped rapidly during the first 100 min and only ~30% of the original PL intensity remained overnight. Although such short surfactants

Figure 4(a) TEM image of the LB assembled monolayer transferred to the copper grid. (b) Fluorescence microscope image of the LB monolayer transferred on a quartz slide. The white dashed line denotes the aligned direction of the NWs. α is the angle between the alignment direction and the polarizer in front of a detector. (c) Polar plots of the relative PL intensities versus the probe polarization angle. Blue line: LB assembled monolayer. Red line: drop-cast film.

are hydrophobic and they can keep most NWs suspended in the organic phase, the NWs still decomposed at the water/oil interface due to the dynamic nature of the ligand binding.

To demonstrate the advantages of PS-P4VP surface modification, we carried out LB assembly of the polymer-protected $CsPbBr_3$ NWs. In the LB technique, a loose nanowire monolayer floats on an aqueous sub-phase, next, controlled uniaxial compression is employed to force the NWs to assemble along the direction normal to the compression (see details in Experimental). After deliberate optimization of the LB assembly parameters, we successfully realized the uniaxial alignment of the NWs in a monolayer, and

transferred it to varying solid substrates (e.g., TEM copper grid in Figure 4a, and quartz slide in Figure 4b). The polarization of the aligned monolayer in Figure 4b was examined by exciting it with 375 nm laser and recording the intensities of the polarized emission at different angles with respect to the NWs alignment direction. A randomly oriented NWs thin film was also made as a control by simply drop-casting the stock nanowire solution on a quartz slide. In Figure 4c, the polar plot of the relative PL intensity as a function of the probe polarizer angle with respect to the assembly direction shows an elliptical shape. The degree of polarization (P), defining as the ratio $P = (I_\parallel - I_\perp)/(I_\parallel + I_\perp)$, was calculated to be 0.36 ± 0.02 ($I_\parallel$ and $I_\perp$ are the intensities of the polarized emission in the directions parallel and normal to the aligned direction of the NWs monolayer, respectively). In contrast, a negligible polarization of 0.021 ± 0.002 was observed in the drop-casting thin film. The polarized emission from the oriented NWs monolayer is attributed to a strong dielectric effect [7] in a single anisotropic NW that is significant since the exciting laser wavelength (375 nm) is much greater than the NW diameter (10 nm). The high degree of NW alignment further emphasizes this effect.

4. Conclusions

In summary, we carried out a chemical modification on colloidal $CsPbBr_3$ nanowires through post-synthetic treatment with an amphiphilic block copolymer PS-P4VP. The resulting nanowires showed a core-shell morphology with enhanced PL emission and stability against water and anion exchange. We further applied the Langmuir-Blodgett technique to assemble monolayers of highly aligned nanowires, and studied their

anisotropic optical properties. Future studies of the post-synthetic NWs treatment by block copolymer will concentrate on changing the molecular weights of each block to tune the shell thickness. We believe that the shell thickness plays an important role in determining the water stability and the anisotropic optical properties of the LB assembly monolayers.

Acknowledgements

Electronic Supplementary Material: Supplementary material is available in the online version of this article at http://dx.doi.org/10.1007/10.1007/s12274-***-****-* (automatically inserted by the publisher) and is accessible free of charge.

References

[1] Dou, L.; Yang, Y.; You, J.; Hong, Z.; Chang, W.-H.; Li, G.; Yang, Y. Solution-Processed Hybrid Perovskite Photodetectors with High Detectivity. *Nat. Commun.* **2014**, *5,* 5404.

[2] Wang, H. C.; Lin, S. Y.; Tang, A. C.; Singh, B. P.; Tong, H. C.; Chen, C. Y.; Lee, Y. C.; Tsai, T. L.; Liu, R. S. Mesoporous Silica Particles Integrated with All-Inorganic Cspbbr3 Perovskite Quantum-Dot Nanocomposites (Mp-Pqds) with High Stability and Wide Color Gamut Used for Backlight Display. *Angew. Chem., Int. Ed.* **2016**, *55,* 7924-7929.

[3] Xiao, Z.; Kerner, R. A.; Zhao, L.; Tran, N. L.; Lee, K. M.; Koh, T.-W.; Scholes, G. D.; Rand, B. P. Efficient Perovskite Light-Emitting Diodes Featuring Nanometre-Sized Crystallites. *Nat. Photonics* **2017**, *11,* 108.

[4] Eaton, S. W.; Lai, M.; Gibson, N. A.; Wong, A. B.; Dou, L.; Ma, J.; Wang, L.-W.; Leone, S. R.; Yang, P. Lasing in Robust Cesium Lead Halide Perovskite Nanowires. *Proc. Natl. Acad. Sci. U.S.A.* **2016**, *113,* 1993-1998.

[5] Lin, J.; Lai, M.; Dou, L.; Kley, C. S.; Chen, H.; Peng, F.; Sun, J.; Lu, D.; Hawks, S. A.; Xie, C.; Cui, F.; Alivisatos, A. P.; Limmer, D. T.; Yang, P. Thermochromic Halide Perovskite Solar Cells. *Nat. Mater.* **2018**, *17,* 261-267.

[6] Huang, H.; Bodnarchuk, M. I.; Kershaw, S. V.; Kovalenko, M. V.; Rogach, A. L. Lead Halide Perovskite Nanocrystals in the Research Spotlight: Stability and Defect Tolerance. *ACS Energy Lett.* **2017**, *2,* 2071-2083.

[7] Wang, J.; Gudiksen, M. S.; Duan, X.; Cui, Y.; Lieber, C. M. Highly Polarized Photoluminescence and Photodetection from Single Indium Phosphide Nanowires. *Science* **2001**, *293,* 1455-1457.

[8] Hu, J.; Li, L.-s.; Yang, W.; Manna, L.; Wang, L.-W.; Alivisatos, A. P. Linearly Polarized Emission from Colloidal Semiconductor Quantum Rods. *Science* **2001**, *292,* 2060-2063.

[9] Boehm, S. J.; Kang, L.; Werner, D. H.; Keating, C. D. Field-Switchable Broadband Polarizer Based on Reconfigurable Nanowire Assemblies. *Adv. Funct. Mater.* **2017**, *27,* 1604703.

[10] Tao, A.; Kim, F.; Hess, C.; Goldberger, J.; He, R.; Sun, Y.; Xia, Y.; Yang, P. Langmuir−Blodgett Silver Nanowire Monolayers for Molecular Sensing Using Surface-Enhanced Raman Spectroscopy. *Nano Lett.* **2003**, *3,* 1229-1233.

[11] Tao, A. R.; Huang, J.; Yang, P. Langmuir−Blodgettry of Nanocrystals and

Nanowires. *Acc. Chem. Res.* **2008**, *41,* 1662-1673.

[12] Kang, J.; Wang, L.-W. High Defect Tolerance in Lead Halide Perovskite Cspbbr3. *J. Phys. Chem. Lett.* **2017**, *8,* 489-493.

[13] Luo, B.; Pu, Y. C.; Lindley, S. A.; Yang, Y.; Lu, L.; Li, Y.; Li, X.; Zhang, J. Z. Organolead Halide Perovskite Nanocrystals: Branched Capping Ligands Control Crystal Size and Stability. *Angew. Chem., Int. Ed.* **2016**, *55,* 8864-8868.

[14] Sun, S.; Yuan, D.; Xu, Y.; Wang, A.; Deng, Z. Ligand-Mediated Synthesis of Shape-Controlled Cesium Lead Halide Perovskite Nanocrystals Via Reprecipitation Process at Room Temperature. *ACS Nano* **2016**, *10,* 3648-3657.

[15] De Roo, J.; Ibáñez, M.; Geiregat, P.; Nedelcu, G.; Walravens, W.; Maes, J.; Martins, J. C.; Van Driessche, I.; Kovalenko, M. V.; Hens, Z. Highly Dynamic Ligand Binding and Light Absorption Coefficient of Cesium Lead Bromide Perovskite Nanocrystals. *ACS Nano* **2016**, *10,* 2071-2081.

[16] Zhang, H.; Wang, X.; Liao, Q.; Xu, Z.; Li, H.; Zheng, L.; Fu, H. Embedding Perovskite Nanocrystals into a Polymer Matrix for Tunable Luminescence Probes in Cell Imaging. *Adv. Funct. Mater.* **2017**, *27,* 1604382.

[17] Raja, S. N.; Bekenstein, Y.; Koc, M. A.; Fischer, S.; Zhang, D.; Lin, L.; Ritchie, R. O.; Yang, P.; Alivisatos, A. P. Encapsulation of Perovskite Nanocrystals into Macroscale Polymer Matrices: Enhanced Stability and Polarization. *ACS Appl. Mater. Interfaces* **2016**, *8,* 35523-35533.

[18] Huang, H.; Chen, B.; Wang, Z.; Hung, T. F.; Susha, A. S.; Zhong, H.; Rogach, A. L. Water Resistant Cspbx3 Nanocrystals Coated with Polyhedral Oligomeric Silsesquioxane and Their Use as Solid State Luminophores in All-Perovskite White Light-Emitting Devices. *Chem. Sci.* **2016**, *7,* 5699-5703.

[19] Zhang, D.; Yu, Y.; Bekenstein, Y.; Wong, A. B.; Alivisatos, A. P.; Yang, P. Ultrathin Colloidal Cesium Lead Halide Perovskite Nanowires. *J. Am. Chem. Soc.* **2016**, *138,* 13155-13158.

[20] Zhang, D.; Yang, Y.; Bekenstein, Y.; Yu, Y.; Gibson, N. A.; Wong, A. B.; Eaton, S. W.; Kornienko, N.; Kong, Q.; Lai, M.; Alivisatos, A. P.; Leone, S. R.; Yang, P. Synthesis of Composition Tunable and Highly Luminescent Cesium Lead Halide Nanowires through Anion-Exchange Reactions. *J. Am. Chem. Soc.* **2016**, *138,* 7236-7239.

[21] Curtis, N. F. Macrocyclic Coordination Compounds Formed by Condensation of Metal-Amine Complexes with Aliphatic Carbonyl Compounds. *Coord. Chem. Rev.* **1968**, *3,* 3-47.

[22] Noel, N. K.; Abate, A.; Stranks, S. D.; Parrott, E. S.; Burlakov, V. M.; Goriely, A.; Snaith, H. J. Enhanced Photoluminescence and Solar Cell Performance Via Lewis Base Passivation of Organic–Inorganic Lead Halide Perovskites. *ACS Nano* **2014**, *8,* 9815-9821.

[23] Koscher, B. A.; Swabeck, J. K.; Bronstein, N. D.; Alivisatos, A. P. Essentially Trap-Free Cspbbr3 Colloidal Nanocrystals by Postsynthetic Thiocyanate Surface Treatment. *J. Am. Chem. Soc.* **2017**, *139,* 6566-6569.

[24] Zhang, D.; Eaton, S. W.; Yu, Y.; Dou, L.; Yang, P. Solution-Phase Synthesis of Cesium Lead Halide Perovskite Nanowires. *J. Am. Chem. Soc.* **2015**, *137,* 9230-9233.

[25] Dursun, I.; De Bastiani, M.; Turedi, B.; Alamer, B.; Shkurenko, A.; Yin, J.; Gereige, I.; Alsaggaf, A.; Mohammed, O. F.; Eddaoudi, M.; Bakr, O. M. Cspb2br5 Single Crystals: Synthesis and Characterization. *ChemSusChem* **2017**, *10,* 3746-3749.

[26] Zuo, L.; Guo, H.; deQuilettes, D. W.; Jariwala, S.; De Marco, N.; Dong, S.; DeBlock, R.; Ginger, D. S.; Dunn, B.; Wang, M.; Yang, Y. Polymer-Modified Halide Perovskite Films for Efficient and Stable Planar Heterojunction Solar Cells. *Sci. Adv.* **2017**, *3*.